Angewandte Chemie
Eine Zeitschrift der Gesellschaft Deutscher Chemiker

Supporting Information

© Wiley-VCH 2007

69451 Weinheim, Germany

Structural Basis for the Activity of the Microtubules Stabilizing Agent Epothilone studied by NMR Spectroscopy in Solution.

Marcel Reese,[1§] Víctor M. Sánchez-Pedregal,[1§] Karel Kubicek,[1] Jens Meiler,[2] Marcel J.J. Blommers,[3] Christian Griesinger,[1*] Teresa Carlomagno[1*]

[1] Department of NMR based Structural Biology, Max Planck Institute for Biophysical Chemistry, Am Fassberg 11, 37077 Göttingen, Germany

[2] Vanderbilt University, Center for Structural Biology, 654 21st Ave South, BIOSCI/MRBIII, Nashville, TN 37212, USA

[3] Novartis Institutes for BioMedical Research, P.O. Box, CH-4002 Basel, Switzerland

~~Supporting Information~~

The sample. Tubulin extracted from bovine brain was purchased from Cytoskeleton Inc. (Denver, CO, USA). 66 µl of tubulin solution were diluted in 350 µl NMR buffer (aqueous solution containing 1.5 mM phosphate, 1.5 mM calcium and sodium at pH 7.0) and dialyzed twice with 1.5 L buffer at 4°C. The solution was dialyzed further with 2 × 15 ml D_2O buffer to exchange H_2O for D_2O.

The NMR sample consisted of epothilone A (EpoA, 0.6 mM), baccatin III (BacIII, 0.6 mM) and tubulin (12µM) in D_2O containing 3 mM phosphate, 1.5 mM calcium and ca. 0.7 mM sodium at pH 7.0. In these conditions and in the absence of both EpoA and BacIII, no microtubules are formed. Tubulin exists in the form of inhomogeneous "aggregates" of α,β – dimers, as observed by electron microscopy (EM) and size-exclusion chromatography (Fig. S1A). Due to the absence of ordered, microtubule-like polymers, we refer to this state as to the non-polymerized, soluble form of tubulin. The addition of EpoA promotes polymerization of tubulin in the form of "microtubule sheets" or "open microtubules" (Fig. S1B). These ordered polymers are like

microtubules that are not closed into the typical cylindrical form. Similar polymers have also been observed in microtubules preparations stabilized by epothilone, as reported by Höfle and coworkers (GBF Scientific Reports, 2005), stabilized by paclitaxel, as reported by Diaz and Andreu[1] and in GMPCPP microtubules formed at low temperature[2]. The protofilaments are here associated in a parallel way, as opposed to the Zn-stabilized sheets, where the protofilaments are antiparallel to each other. It is likely that MT-sheets are formed instead of MTs due to the presence of Ca^{2+} and to the absence of Mg^{2+}. The observation that epothilone induces the reorganization of the non-polymerized tubulin into ordered polymers indicates that the drug binds to the non-polymerized tubulin and induces the protein conformational change necessary for the formation of the elongated polymers. While it is known that epothilones bind much tighter to microtubules than to soluble tubulin,[3] our data demonstrate that epothilone functionally binds to non-polymerized tubulin, inducing formation of ordered polymers, even in absence of Mg^{2+} and GTP and in the presence of Ca^{2+}. The structural data discussed in this work refer to epothilone bound to the soluble, non-polymerized tubulin form. The amount of epothilone bound to the microtubule sheets (Fig. S1B) does not contribute to the NMR signal. This is due to the fact that only signals from fast exchanging ligands can be observed in the NMR experiments, while epothilones are known to bind tightly to microtubules.[3] In agreement with this consideration we do not observe any change in the EpoA NOE signals with time, whereas the microtubule sheets precipitate out of solution in a few days.

INPHARMA Measurements. We measured intermolecular NOEs between epothilone EpoA and BacIII in the presence of tubulin (Fig. 1C). The complex EpoA/tubulin or BacIII/tubulin are only transiently formed during the mixing time of a NOESY experiment, and transferred-NOEs (tr-NOEs) can be observed in a 50:1 mixture of EpoA and tubulin or BacIII and tubulin (K_d in the micromolar range for both complexes).

We recorded NOESY experiments at different mixing times (20, 40, 70, 100 and 200 ms) on a Bruker 900 MHz spectrometer. Nineteen intermolecular NOE peaks can be already observed in a NOESY experiment at 40 ms mixing time. The normalized intensities at four different mixing times for all observed intermolecular NOEs are reported in Table S1.

The principle underlying the observation of intermolecular NOEs between two ligands binding competitively and consecutively to a common protein has been described in a previous publication.[4] Briefly, an NOE peak between a proton H_A of ligand A and a proton H_B of ligand B in the presence of the receptor T originates from spin diffusion involving a proton H_T of the receptor. During the NOESY mixing time the ligand A binds to T and proton H_A transfers its magnetization to proton H_T. Then the complex TA dissociates and B binds to T. The magnetization of H_A, which had been transferred to H_T, can now be transferred to H_B, resulting in an intermolecular peak H_A-H_B. Clearly, this peak can only exist if both H_A and H_B are close to H_T in the TA and TB complexes, respectively. Therefore, a number of such intermolecular NOE peaks describe the relative orientation of the two ligands in the receptor binding pocket. In our previous publication,[4] we proposed to rank docking modes of the ligands A and B to the common target T by evaluating their compatibility with the experimental interligand NOEs. We called this new methodology INPHARMA (*I*nterligand *N*OEs for *Phar*macophore *Ma*pping). Here we apply this approach to the determination of the binding modes of EpoA and BacIII to non-polymerized tubulin.

The build-up curves of the intensities of the intermolecular NOE peaks between EpoA and BacIII in the presence of tubulin show the characteristic parabolic shape for spin-diffusion-mediated NOE effects.[4] As a control, we recorded a NOESY spectrum of the mixture of EpoA and BacIII in the absence of tubulin at 400 ms mixing time, which showed no intermolecular NOEs. Thus, we can conclude that the intermolecular NOE effects between EpoA and BacIII, observed in the presence of tubulin, are mediated by protons of tubulin.

Docking calculations. 5315 EpoA/β-tubulin and 5022 BacIII/β-tubulin complex models were generated with the HADDOCK protocol [5] using the CNS program.[6] To improve the sampling of the conformational space of tubulin, seven and fourteen initial β-tubulin models were used for generating the EpoA/tubulin and the BacIII/tubulin complex models, respectively. These initial models included the electron crystallography (EC) derived structure of polymerized tubulin bound to paclitaxel (1JFF.pdb) [7] and the EC-derived structure of polymerized tubulin bound to EpoA (1TVK.pdb).[8] The remaining 5 and 12 tubulin models for the EpoA/tubulin and the BacIII/tubulin complexes, respectively, resulted from previous docking calculations of

EpoA and BacIII to tubulin and belonged to complex models where the ligands are found in very different orientations in the binding pocket.

Increasing flexibility was allowed for the protein during the docking protocol. After a first stage of rigid docking, structural models were selected having the ligand close to the taxane binding pocket. In the following stages, we allowed the protein side chains in the binding pocket and the loop backbone to be flexible. In the last water refinement step full flexibility of the protein was allowed and the complex was hydrated with a water layer of about 8 Å. This procedure was designed to access conformational states of tubulin that could differ to some extent from the conformation of tubulin polymerized in Zn-stabilized sheets.

The conformations of EpoA and BacIII were kept rigid throughout the docking calculation. Methyl and hydroxyl hydrogen atoms were allowed to rotate. For EpoA we used the tubulin-bound conformation determined by tr-NOE and transferred cross-correlated relaxation (tr-CCR) rates in our previous work.[9] These data were complemented with the measurement of the C19-C18-C17-C16 torsion angle through the CH-CH dipolar-dipolar CCR rate between the C19-H19 vector and the C17-H17 vector. As a consequence of the new CCR data, the C19-C18-C17-C16 torsion angle was restrained to the range –40° - +40°. The tubulin-bound conformation of BacIII was verified by tr-NOE data and was found to be equivalent to the conformation of the baccatin core of paclitaxel in the EC-derived structure.[7]

The charges of both ligands were calculated in *vacuo* by MOPAC [10] from Insight II using the MINDO/3 Hamiltonian.[11] As for the protein, implicit hydrogen bonding was introduced for hydrogen donors and acceptors of the ligands. The ligands non-bonded parameters were adapted to fit the PARALLHDG_5.3 parameter set from Michael Nilges (July 07, 2001 University of California) as provided with HADDOCK 1.0.

Intermolecular NOEs calculations. The peak volumes in the mixing time of a NOESY spectrum evolve according to the differential equation:

$$\frac{d\mathbf{A}(t)}{dt} = -(\mathbf{R} + \mathbf{K}) \cdot \mathbf{A}(t) \qquad \text{Eq. 1}$$

where **A** denotes the square matrix of the peak volumes, **R** is the relaxation matrix and **K** the chemical exchange matrix.[12] Solution of Eq. 1 leads to the matrix $\mathbf{A}(t_m)$, which contains the intensities of all peaks in a NOESY spectrum with mixing time t_m. The formal solution is:

$$\mathbf{A}(t_m) = \exp[-(\mathbf{R}+\mathbf{K})\, t_m] \cdot \mathbf{A}(0) \qquad \text{Eq. 2}$$

where $\mathbf{A}(0)$ contains the initial magnetization.

We describe the system with a two-state kinetic model (Scheme S1), where we assume that the concentration of the free protein is negligible due to the large excess of ligands. Four chemical species are considered: free ligand A (EpoA), free ligand B (BacIII), complex TA (EpoA/tubulin) and complex TB (BacIII/tubulin).

$$\mathbf{B + TA} \underset{k_{21}}{\overset{k_{12}}{\rightleftharpoons}} \mathbf{A + TB}$$

Scheme S1

The relaxation matrix **R** contains the relaxation rates between protons in the four distinct molecular species. The general form of the relaxation matrix is:

$\mathbf{R}_A^A$					
	$\mathbf{R}_B^B$				
		$\mathbf{R}_A^{TA}$	$\mathbf{R}_{A,T}^{TA}$		
		$\mathbf{R}_{T,A}^{TA}$	$\mathbf{R}_T^{TA}$		
				$\mathbf{R}_B^{TB}$	$\mathbf{R}_{B,T}^{TB}$
				$\mathbf{R}_{T,B}^{TB}$	$\mathbf{R}_T^{TB}$

The bold lines group the sub-matrices corresponding to each one of the four species in the solution. The superindex of each $\mathbf{R}_x^s$ indicates the species (either the free ligands or the complexes TA or TB) and the subindex indicates which protons of the species contribute to that sub-matrix. Thus, $\mathbf{R}_B^B$ describes the relaxation of the protons of ligand B in the free state and $\mathbf{R}_B^{TB}$ the relaxation of the protons of ligand B when bound in the complex TB. Analogously, $\mathbf{R}_T^{TB}$ describes the relaxation of the protein protons in the complex TB and $\mathbf{R}_{B,T}^{TB}$ contains the cross-relaxation terms between the protons of ligand B and the protons of protein T in the complex TB.

The individual sub-matrices representing each of the four chemical species are symmetric square matrices of dimension $N^s \times N^s$, where N^s is the number of protons considered for each of the four different species s. To reduce the matrix sizes and be able to perform the calculation in a reasonable time, we considered only tubulin atoms within a given distance d from the ligand.

The matrix **K** represents the kinetics of the species in equilibrium and has the same dimension as the relaxation matrix **R**:[12]

k_{21}[TB] **I**		- k_{12}[B] **I**			
	k_{12}[TA] **I**			- k_{21}[A] **I**	
- k_{21}[TB] **I**		k_{12}[B] **I**			
			k_{12}[B]**I**		- k_{21}[A] **I**
	-k_{12}[TA] **I**			k_{21}[A] **I**	
			- k_{12}[B] **I**		k_{21}[A] **I**

I indicates the identity matrix and [A], [B], [TA] and [TB] are the concentrations of the corresponding species.

Structure selection criteria. The theoretical intermolecular NOEs between the two ligands EpoA and BacIII were calculated for each of the 26.7 millions pairs of docking models (5315 for the EpoA/tubulin complex and 5022 for the BacIII/tubulin complex) assuming a k_{off} >> 100 Hz for both complexes. This lower bound of the k_{off} was verified by relaxation dispersion experiments. To reduce the matrix sizes, we considered only tubulin atoms in a distance $d < 8.5$ Å from the ligand. By gradually increasing this limit, we verified that 8.5 Å is the optimal value to obtain reliable interligand NOEs while keeping the calculation time at reasonable values. For complex pairs with a linear correlation coefficient $R > 0.78$, the final interligand NOEs were calculated using a cut off of 20 Å.

The theoretical intermolecular NOEs were compared with the experimental values by a linear regression algorithm. The best pair of models delivered a linear correlation coefficient R of 0.92. Three criteria were applied in the selection of pairs of models: first, the linear correlation coefficient has to exceed 0.86; second, the slope of the regression lines of the experimental *vs.* the calculated data must be between 0.3 and 1.4; third, the slope of the regression line of each intense NOE peak does not exceed two times the slope of the regression line of all the NOE peaks together. The second selection criterion considers that the calculated NOE intensities, normalized to the diagonal peak intensities, should have the same size as the experimental ones. The upper bound was set to 40%. The lower bound allows the experimental NOEs to be 70% smaller than the calculated ones. The logic behind this criterion is based on the presence of internal motions, which could significantly reduce the experimental intermolecular NOEs. Internal motions cannot be simulated in the theoretical calculations, due to the lack of a satisfactory model for such a complex system. However, motion is not likely to increase the NOE by the same amount, which led us to set the upper bound of the slope to 40%.

The 25 million pairs of models were clustered to facilitate the analysis. The pairwise RMSD of models belonging to the same cluster did not exceed 2 Å on EpoA heavy atoms after translation of their geometric center of mass into the origin of the coordinate system. After application of the selection criteria two families of pairs were considered further, pairs A and B. Pair A is represented by the EpoA/tubulin model of Fig. 1 and the BacIII – tubulin model of Fig. S2. Pair B was discarded due to the fact that the

aromatic ring of baccatin in the BacIII/tubulin complex does not occupy any of the pockets where the aromatic rings of PTX are found in the EC-derived model of the PTX/tubulin complex.[7] The orientation of the baccatin core also differs from those found in both the EC-derived [7] and the REDOR/FRET-derived models [13],[14] of the PTX/ tubulin complex. In summary, the binding mode of BacIII to tubulin in pair B contradicts the structural data available for the interaction of taxanes with tubulin and was not considered further.

The EpoA/tubulin and BacIII/tubulin models of pair A were further refined through 230 ps of molecular dynamics, which improved the correlation coefficient by 0.02.

The BacIII/tubulin model. The model of the BacIII/tubulin complex that provides a good fit of the experimental interligand NOEs with the EpoA/tubulin complex model of Fig. 1, is shown in Fig. S2. In contrast to our expectation, the baccatin binding mode obtained by the EC-derived PTX/tubulin complex,[7] after removal of the side chain on C13, does not fit the experimental interligand NOE data in combination with any of the EpoA/tubulin complex models (R = 0.75). Instead, docking models where baccatin places the C2 benzoyl phenyl ring in the pocket occupied by the C3' phenyl in the PTX – tubulin complex, close to F270, are consistent with the INPHARMA data. The orientation of the baccatin core in the BacIII/tubulin complex of Fig. S2, however, is similar to the one proposed for the PTX/tubulin complex on the basis of FRET and REDOR data.[14, 15] The fact that the binding mode of baccatin to tubulin differs from the one of paclitaxel is not surprising, considering that baccatin lacks the C3' benzamido phenyl, which plays a fundamental role in the determination of the binding mode of PTX to tubulin by interacting with H227. It should be noted that our model of the BacIII/ tubulin complex explains the enhanced activity of 2-*m*-azido baccatin by invoking the interaction of the azido group with the guanidinium group of R320.[15] However, we do not exclude that 2-*m*-azido baccatin might have a binding mode that differs from that of baccatin, as allowed by the broad and flexible tubulin binding pocket and in agreement with the large difference in their biological activity.[16]

The EpoA/tubulin model. In the main body of this paper we discuss how the model of Fig. 1 can explain several SAR data available for the epothilone/tubulin complex. Here we extend this discussion to two additional pieces of data.

First, SAR data on epimers of 14-methyl EpoB and EpoD show that the *R* configuration for EpoB and the *S* configuration for EpoD retain most of the biological activity while the respective *S* and *R* configurations are inactive.[17, 18] In agreement with these data, 14-methyl EpoB with *S* configuration at the C14 could not adopt the NMR-derived bioactive conformation due to steric hindrance with the Me27 and the H11 proton. Analogously, introduction of a methyl group at the C10 with *S* configuration leads to inactive EpoC, as expected from the steric clash of this additional methyl group with the protons at the C2.

Second, the (*E*)-9,10-dehydro- and (*E*)-10,11-dehydro- analogues have been found to retain the biological activity of epothilone,[19, 20] in agreement with the *trans* disposition around the C9-C10 and C10-C11 torsion angles of the NMR-derived bioactive conformation.[9] In contrast, in the EC-derived structure the C10-C11 torsion angle is close to 90°.

Additionally, the EpoA/tubulin complex shown in Fig. 1 well explains saturation transfer difference[21] (STD) data, which show a strong decrease of the NMR signals of EpoA in the C13-C21 region upon saturation of tubulin resonances. This data identify the C13-C21 region as the one in close contact with the protein, which is in very good agreement with the structure of Fig. 1.

Table S1: List of the intensities of the intermolecular NOEs between protons of baccatin III and epothilone A in the presence of tubulin at four mixing times. B and E indicate baccatin and epothilone, respectively. B-o, B-m, B-p indicate the protons in the *orto*-, *meta*- and *para*- positions of the C2 benzoyl phenyl ring of baccatin. The NOE intensities are normalized relative to the diagonal peak intensity of proton A and multiplied by 10^4.

		NOESY mixing times			
Proton A	Proton B	40ms	70ms	100ms	200ms
B-m	E-21	8	14	26	68
B-p	E-21	9	10	25	81
B-o	E-21	4	12	19	60
E-21	B-16	8	9	15	50
E-21	B-17	5	11	17	65
B-m	E-27	5	16	24	70
B-p	E-27	4	17	23	75
B-o	E-27	3	10	22	65
B-m	E-22	5	13	20	57
B-p	E-22	3	10	14	61
B-o	E-22	5	10	16	50
B-m	E-23	4	9	19	50
B-p	E-23	0	7	18	53
B-o	E-23	4	8	15	43
B-m	E-25	4	15	19	66
B-p	E-25	7	14	21	72
B-o	E-25	3	12	21	57
E-19	B-16	8	13	24	62
E-19	B-17	10	16	23	85
B-10	E-25	0	7	9	48
B-3	E-22	0	7	14	49
B-5	E-22	5	9	14	41
E-15	B-17	9	15	24	82
E-17	B-17	12	21	25	78
E-15	B-16	6	15	30	67
B-5	E-24	0	0	9	31
B-m	E-24	3	13	19	49
B-p	E-24	0	9	11	56
B-o	E-24	3	7	14	44
B-5	E-23	0	4	9	40
B-2	E-23	0	4	9	17
B-10	E-23	0	5	9	26
B-13	E-27	0	6	19	64
B-5	E-27	2	7	8	43
B-2	E-27	0	7	7	35
B-10	E-21	4	11	12	34
B-13	E-21	0	7	9	31

B-o	E-12	4	3	9	21
B-o	E-13	0	3	4	24
B-m	E-7	0	3	6	16
B-o	E-7	0	3	4	15
B-m	E-15	0	0	6	22
E-21	B-2	0	1	7	19
B-5	E-17	0	0	5	13
B-2	E-17	0	0	0	18
B-m	E-17	0	5	6	22
B-p	E-17	0	0	6	22
B-o	E-17	0	5	6	17
B-m	E-19	0	6	12	29
B-o	E-19	0	5	9	20
E-15	B-o	6	16	28	69

Figures and Legends

A **B**

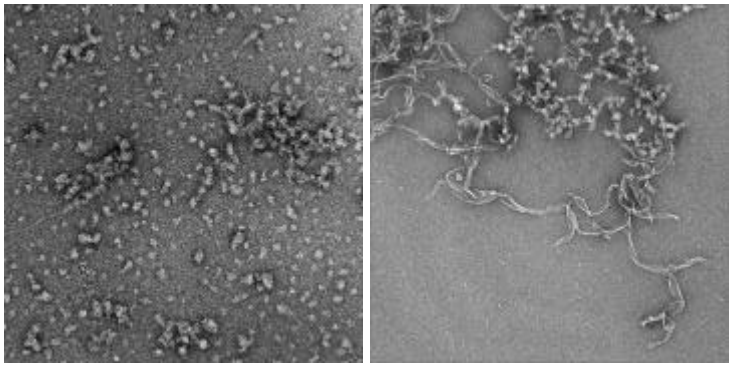

Fig. S1 Electron microscopy (EM) images of tubulin (12μM) dissolved in a D_2O solution containing 3 mM phosphate, 1.5 mM calcium and ca. 0.7 mM sodium at pH 7.0 (panel **A**). In panel **B** the same tubulin sample was incubated for 1 hour with 0.6 mM epothilone A, leading to the formation of ordered polymers (microtubule sheets).

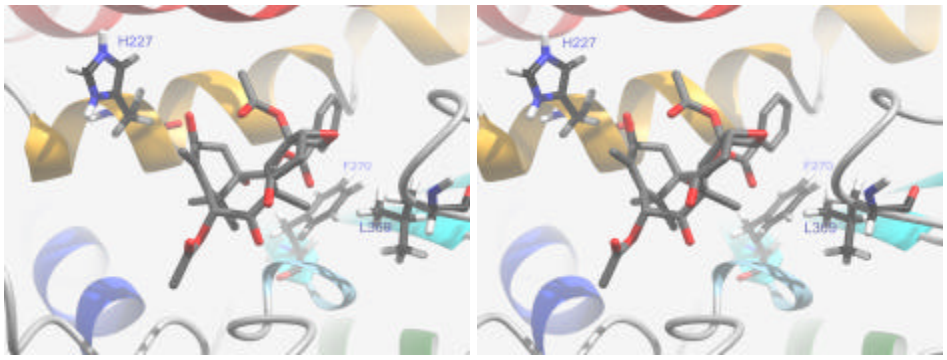

Fig. S2 Model of the BacIII/tubulin complex that best reproduces the experimental interligand NOEs in combination with the EpoA/tubulin complex of Fig. 1. The orientation of the baccatin core differs from the one observed in the EC-derived model of the PTX/tubulin complex[7] and is similar to that proposed on the basis of FRET and REDOR data.[14, 15] The C2 benzoyl phenyl is situated in the hydrophobic pocket defined by F270 and L369, where paclitaxel places the C3' phenyl in the EC-derived complex model. [7]

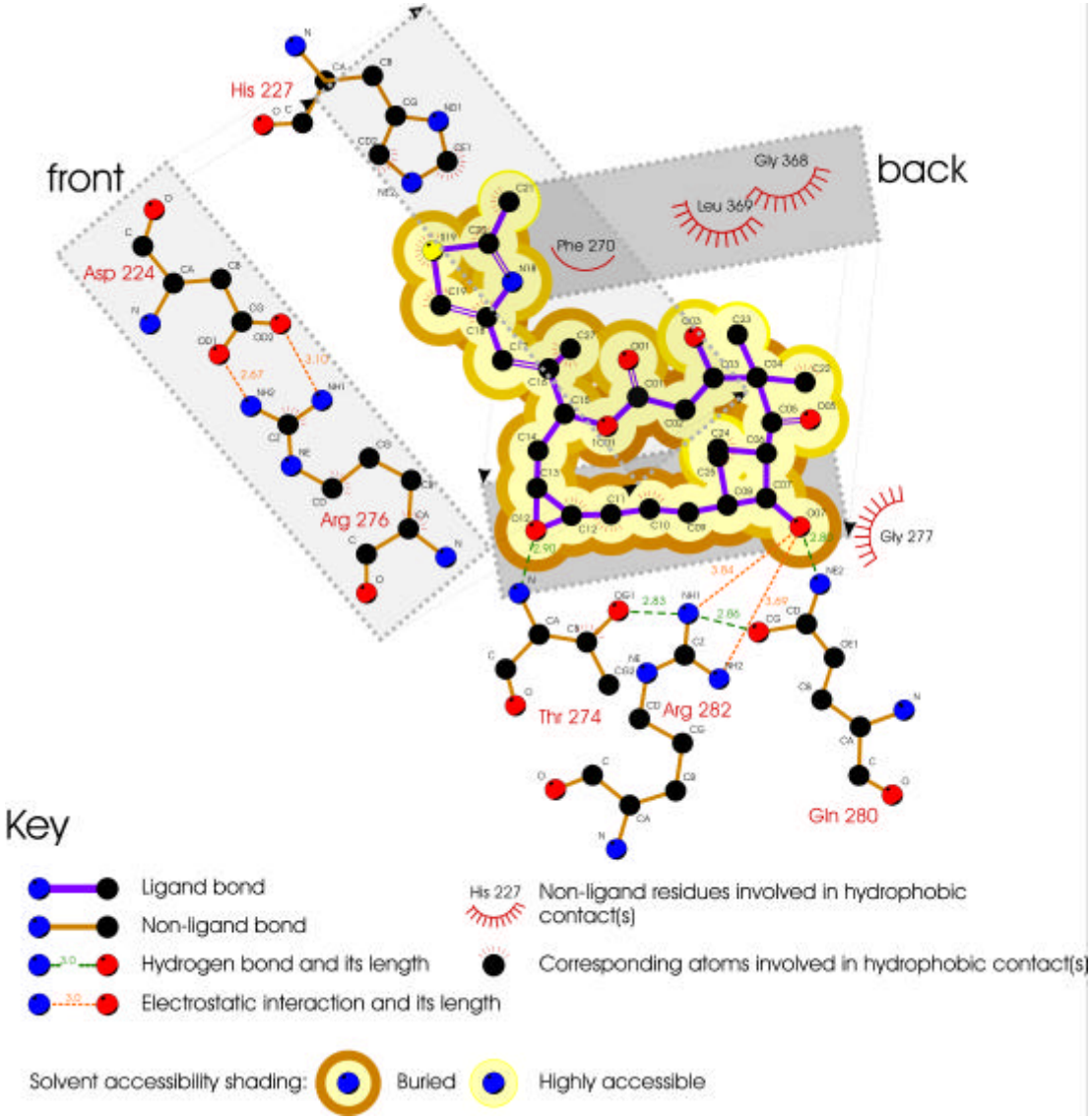

Fig. S3 Schematic 2D view of the electrostatic and hydrophobic contacts of epothilone to tubulin. The symbols used are explained in the figure.

Fig. S4 View of the model of the EpoA/tubulin complex of Fig. 1, which shows the hydrophobic interactions of the EpoA stretch C9-C12 with the leucine-rich floor of the binding pocket including P272, L273, L284 and L369. The epoxide ring is situated at the entrance of the hydrophobic pocket occupied by F270.

[1] J. F. Diaz, J. M. Andreu, *Biochemistry* **1993**, *32*, 2747.
[2] H. W. Wang, E. Nogales, *Nature* **2005**, *435*, 911.
[3] R. M. Buey, J. F. Diaz, J. M. Andreu, A. O'Brate, P. Giannakakou, K. C. Nicolaou, P. K. Sasmal, A. Ritzen, K. Namoto, *Chem. Biol.* **2004**, *11*, 225.
[4] V. M. Sanchez-Pedregal, M. Reese, J. Meiler, M. J. Blommers, C. Griesinger, T. Carlomagno, *Angew. Chem. Int. Ed. Engl.* **2005**, *44*, 4172.
[5] C. Dominguez, R. Boelens, A. M. Bonvin, *J. Am. Chem. Soc.* **2003**, *125*, 1731.
[6] A. T. Brunger, P. D. Adams, G. M. Clore, W. L. DeLano, P. Gros, R. W. Grosse-Kunstleve, J. S. Jiang, J. Kuszewski, M. Nilges, N. S. Pannu, R. J. Read, L. M. Rice, T. Simonson, G. L. Warren, *Acta Crystallogr. D Biol. Crystallogr.* **1998**, *54*, 905.
[7] E. Nogales, S. G. Wolf, K. H. Downing, *Nature* **1998**, *391*, 199.
[8] J. H. Nettles, H. Li, B. Cornett, J. M. Krahn, J. P. Snyder, K. H. Downing, *Science* **2004**, *305*, 866.
[9] T. Carlomagno, M. J. Blommers, J. Meiler, W. Jahnke, T. Schupp, F. Petersen, D. Schinzer, K. H. Altmann, C. Griesinger, *Angew. Chem. Int. Ed. Engl.* **2003**, *42*, 2511.
[10] J. J. P. Stewart, *J. Comp. Aid. Mol. Des.* **1990**, *4*, 1.
[11] R. C. Bingham, M. J. S. Dewar, D. H. Lo, *J. Am. Chem. Soc.* **1975**, *97*, 1285.
[12] F. Ni, *J. Magn. Reson. Series B* **1995**, *106*, 147.
[13] F. Ni, *J. Magn. Reson., Series B* **1996**, *106*, 147.
[14] Y. Li, B. Poliks, L. Cegelski, M. Poliks, Z. Gryczynski, G. Piszczek, P. G. Jagtap, D. R. Studelska, D. G. Kingston, J. Schaefer, S. Bane, *Biochemistry* **2000**, *39*, 281.
[15] M. T. Ivery, T. Le, *Oncol. Res.* **2003**, *14*, 1.
[16] L. He, P. G. Jagtap, D. G. Kingston, H. J. Shen, G. A. Orr, S. B. Horwitz, *Biochemistry* **2000**, *39*, 3972.

[17] R. E. Taylor, Y. Chen, A. Beatty, D. C. Myles, Y. Zhou, *J. Am. Chem. Soc.* **2003**, *125*, 26.
[18] R. E. Taylor, Y. Chen, G. M. Galvin, P. K. Pabba, *Org. Biomol. Chem.* **2004**, *2*, 127.
[19] A. Rivkin, F. Yoshimura, A. E. Gabarda, T. C. Chou, H. Dong, W. P. Tong, S. J. Danishefsky, *J. Am. Chem. Soc.* **2003**, *125*, 2899.
[20] I. H. Hardt, H. Steinmetz, K. Gerth, F. Sasse, H. Reichenbach, G. Höfle, *J. Nat. Prod.* **2001**, *64*, 847.
[21] M. Mayer, B. Meyer, *J. Am. Chem. Soc.* **2001**, *123*, 6108.